

Competition between lithium and magnesium ions for the G-protein transducin in the guanosine 5'-diphosphate bound conformation

Chandra Srinivasan ^{a,b}, Jason Toon ^a, Louis Amari ^a, Abde M. Abukhdeir ^a, Heidi Hamm ^c, Carlos F.G.C. Geraldès ^d, Yee-Kin Ho ^e, Duarte Mota de Freitas ^{a,*}

^a Department of Chemistry, Loyola University Chicago, 6525 N. Sheridan Road, Chicago, IL 60626, USA

^b Department of Chemistry and Biochemistry, California State University, Fullerton, CA 92834, USA

^c Department of Pharmacology, Vanderbilt University, Nashville, TN 37232, USA

^d Department of Biochemistry and Center of Neurosciences, University of Coimbra, P.O. Box 3126, 3001-401 Coimbra, Portugal

^e Department of Biochemistry and Molecular Biology, University of Illinois at Chicago, Chicago, IL 60499, USA

Received 23 September 2003; received in revised form 29 December 2003; accepted 31 December 2003

Abstract

Li⁺ is the most effective drug used to treat bipolar disorder; however, its exact mechanism of action has yet to be elucidated. One hypothesis is that Li⁺ competes with Mg²⁺ for the Mg²⁺ binding sites on guanine-nucleotide binding proteins (G-proteins). Using ⁷Li T₁ relaxation measurements and fluorescence spectroscopy with the Mg²⁺ fluorophore furaptra, we detected Li⁺/Mg²⁺ competition in three preparations: the purified G-protein transducin (G_t), stripped rod outer segment membranes (SROS), and SROS with purified G_t reattached (ROS-T). When purified ROS-T, SROS or transducin were titrated with Li⁺ in the presence of fixed amounts of Mg²⁺, the apparent Li⁺ binding constant decreased due to Li⁺/Mg²⁺ competition. Whereas for SROS the competition mechanism was monophasic, for G_t, the competition was biphasic, suggesting that in G_t, Li⁺/Mg²⁺ competition occurred with different affinities for Mg²⁺ in two types of Mg²⁺ binding sites. Moreover, as [Li⁺] increased, the fluorescence excitation spectra of both ROS-T and G_t were blue shifted, indicating an increase in free [Mg²⁺] compatible with Li⁺ displacement of Mg²⁺ from two low affinity Mg²⁺ binding sites of G_t. G_t release from ROS-T membrane was also inhibited by Li⁺ addition. In summary, we found evidence of Li⁺/Mg²⁺ competition in G_t-containing preparations.

© 2004 Elsevier Inc. All rights reserved.

Keywords: Transducin; G-proteins; Lithium; Magnesium; Ionic competition

1. Introduction

For 50 years, Li⁺ has been the most effective treatment for bipolar disorder, despite the fact that its pharmacological mechanism of action remains unknown. Several hypotheses for its mechanism of action have been advanced [1–3]. One main branch of the research into the Li⁺ mechanism of action has focused on the effect of Li⁺ on guanine-nucleotide binding (G) proteins.

G-proteins are membrane-bound proteins, which play a vital role in cellular communication [4,5]. They function as molecular switches by relaying extracellular signals to specific intracellular effectors [4,5]. Thus, G-proteins affect the way cells interact with their environment, which is critical to the overall health and viability of an organism.

Some studies have provided evidence for the presence of hyperfunctional G-proteins or for abnormal amounts of G-proteins in the membranes of bipolar patients relative to those present in normal individuals [6,7]. Another study found that therapeutic concentrations of Li⁺ inhibited the activities of G_t and G_s (two G-proteins that inhibit and stimulate, respectively), the enzyme

* Corresponding author. Tel.: +1-773-508-3091/3149; fax: +1-773-508-3086.

E-mail address: dfreita@luc.edu (D.M. de Freitas).

adenylate cyclase, and G_q and G_o (G-proteins that regulate phosphatidyl inositol (PI) turnover via the modulation of the activity of phospholipase C) [8]. Li^+ inhibition of these G-proteins affects the ability of various neurotransmitters to bring about a cellular response by decreasing the G-protein-regulated production of the second messenger molecules: cAMP, DAG or IP_3 [3]. Thus, the therapeutic effect of Li^+ may be due to Li^+ inhibition of the G-proteins that are involved in the regulation of adenylate cyclase (G_s and G_i) and of PI turnover (G_q and G_o) as well as by the $G_{\beta\gamma}$ dimer via modulation of the production of the aforementioned second messenger molecules [3,8–12].

One ionic hypothesis as to how Li^+ is able to provide this mood regulation in bipolar patients is that Li^+ competes with Mg^{2+} for the Mg^{2+} binding sites in G-proteins. It is known that G-proteins have at least two types of Mg^{2+} binding sites – specifically, a high affinity Mg^{2+} binding site (K_d value in the nM range) that is needed for the hydrolysis of GTP and a low affinity Mg^{2+} binding site(s) (K_d value(s) in the mM range) that is required for the hormone-catalyzed GDP/GTP exchange [5]. Because Li^+ and Mg^{2+} ions have similar chemical and physical properties [13], competition between Li^+ and Mg^{2+} for the Mg^{2+} binding sites present in G-proteins could occur. Avissar et al. [14] hypothesized that competition between Li^+ and Mg^{2+} ions may occur for the low-affinity Mg^{2+} -binding sites in the G proteins present in the membranes from rat cerebral cortex, and indeed found that increasing the Mg^{2+} concentration reversed the inhibitory effect of Li^+ on G_s , G_i and G_o . Using these observations as a basis for the current investigation, we tested the Li^+ and Mg^{2+} competition hypothesis as a possible mechanism of Li^+ action using two complimentary spectroscopic methods (7Li NMR spectroscopy and fluorescence spectroscopy with the Mg^{2+} -sensitive fluorophore furaptra) for three model G-protein-containing preparations. The G-protein used in our study was transducin (G_t), which is bound on the rod outer segment (ROS) membrane. Therefore, we chose to purify G_t , stripped ROS membranes (SROS), where all peripheral membrane proteins, including G_t , were removed, and SROS membranes with purified G_t reattached.

These biophysical studies (particularly NMR), required large amounts of protein (10–20 mg); therefore we chose to use G_t as our model system since it was possible to purify 20–30 mg of protein quickly and easily, following a published procedure [15]. Additionally, the ROS membrane, in which G_t is normally embedded, can also be quickly and easily isolated, allowing the construction of a reconstituted membrane system [15]. Considering the fact that the amino acids involved in high-affinity Mg^{2+} coordination are essentially the same in most of the proteins in the G-protein superfamily [16–21], whereas those involved in low-affinity

Mg^{2+} binding are unknown, it is important to determine whether the metal ion competition results obtained in our study may be extended to other G-proteins.

Like all G-proteins, G_t acts as a molecular switch. Specifically, G_t is involved in regulating a light-activated cGMP cascade in the ROS membranes of vertebrate rod photoreceptor cells [5,15]. In its inactive conformation, G_t has GDP is bound to the α subunit of G_t ($G_{t\alpha}$ -GDP) and is tightly associated to its $G_{t\beta\gamma}$ complex. Upon photoexcitation, photoexcited rhodopsin (R^*) promotes GTP/GDP exchange, transforming G_t from its inactive GDP-bound form into its active GTP-bound form. $G_{t\alpha}$ -GTP then dissociates from the R^* - $G_{t\beta\gamma}$ complex and activates a cGMP phosphodiesterase (PDE). The intrinsic GTPase activity of the $G_{t\alpha}$ subunit hydrolyzes GTP to GDP, at which point $G_{t\alpha}$ -GDP reassociates with the $G_{t\beta\gamma}$ complex, allowing G_t to relay another extracellular signal [5,15].

The inactive conformation of G_t , G_t -GDP, was chosen as a starting point for our examination of the competition between Li^+ and Mg^{2+} for the Mg^{2+} binding sites in G_t because the high-affinity Mg^{2+} binding site of G_t has been shown, by X-ray crystallographic studies, to be more exposed in this conformation than in the active conformation [19]. Specifically, for G_t in the inactive conformation, the X-ray crystallographic studies have shown that the octahedrally-coordinated Mg^{2+} ion is bound to four water molecules, to the β -phosphate of GDP and to the side chain oxygen of Ser 43 [19]. On the other hand, for G_t in the GTP-bound conformation, the Mg^{2+} ion is coordinated to the side chain oxygens of Thr 177 and Ser 43, to the β and γ phosphates of GTP and to only 2 molecules of water [19]. Thus, in the GTP-bound conformation, the Mg^{2+} ion is less accessible to the aqueous milieu than in the GDP-bound conformation [19]. Therefore, Li^+ / Mg^{2+} competition for the Mg^{2+} binding sites of G_t may be more readily observable in its inactive GDP-bound form than in its active GTP-bound form.

2. Experimental

2.1. Materials

G_t and SROS membranes were isolated from bovine eyes collected at local packing companies. All biochemicals and inorganic salts were purchased from Sigma Chemical Company (St. Louis, MO). Furaptra was purchased from Molecular Probes (Eugene, OR). The Bio-Rad Bradford dye reagent used for protein determinations was purchased from Bio-Rad Laboratories (Hercules, CA), while the gels and buffer strips used for sodium dodecyl sulfate polyacrylamide gel electrophoresis (SDS-PAGE) analysis were purchased from Pharmacia Biotech (Uppsala, Sweden).

2.2. Preparation of purified G_t and SROS membranes from bovine retinas

G_t and SROS membranes were prepared from fresh bovine eyes as described in the literature [15] with the following modification: 100 μ l of 10 mM GTP instead of 50 μ l was added to each tube that contained G_t bound to ROS membrane to ensure that sufficient GTP was present to allow G_t to dissociate from the rhodopsin in the ROS membranes. The purity of the G_t was assessed by SDS-PAGE using a Pharmacia Phase system, while the protein concentration was determined by the Bradford method using the Bio-Rad Bradford dye with bovine serum albumin as a standard [22]. For protein concentration determinations of preparations of G_t bound to SROS membranes, a modified protein analysis procedure using detergent was used [23]. A typical G_t isolation from 400 bovine retinas usually yielded 20–30 mg of pure protein, which is consistent with previous reports [15].

2.3. Preparation of G_t samples for fluorescence, NMR and G_t release experiments

A preparation of apo G_t was required for this investigation to ensure that the majority of the Mg^{2+} in the system was the Mg^{2+} that was added during the NMR, fluorescence, and G_t release experiments, rather than the excess Mg^{2+} (2 mM) that is generally present at the end of a G_t isolation. To remove any excess, unbound Mg^{2+} and any other metal ion contaminants (especially paramagnetic ions that would affect the 7Li T_1 relaxation measurements), the G_t preparations were dialyzed against 50 mM tris[hydroxymethyl] amino-methane hydrochloride (Tris/HCl; pH 7.5). To remove Mg^{2+} tightly bound to the protein, the G_t samples were dialyzed against a buffered solution containing 50 mM Tris/HCl (pH 7.5), 0.1 M NaCl, 0.01% *n*-octyl- β -D-glucopyranoside, 5 mM dithiothreitol (DTT), 0.03 mM GDP, and 1 mM ethylenediamine-*N,N,N',N'*-tetraacetic acid (EDTA), changing the buffer twice over a six hour period [24]. The samples were then dialyzed for 24 h changing the buffer three times against 50 mM Tris/HCl (pH 7.5), 0.1 M NaCl, and 0.03 mM GDP in order to allow the protein to refold in the GDP-bound conformation and to remove any excess EDTA. Following the Mg^{2+} removal, the protein samples were concentrated using an Amicon ultrafiltration cell with a YM-10 membrane, to the desired concentrations of 0.1 mM for both the NMR and fluorescence experiments, or 5 μ M for the G_t release assays.

To verify the removal of all metal ions including Mg^{2+} , several samples were sent to the Chemical Analysis Laboratory, University of Georgia, Athens, GA, for analysis on an inductively coupled plasma emission spectrometer (ICP-ES). The ICP-ES analysis showed

that a very small amount of Mg^{2+} was still present, with a concentration of approximately 10% of the protein concentration. The ICP-ES analysis also showed indirectly that the concentration of phosphorous in the sample was approximately equal to twice that of the protein concentration in the sample suggesting that GDP was bound to the protein in a 1:1 ratio, since there are two phosphorus atoms per GDP molecule.

For the NMR experiments, the Mg^{2+} -free G_t samples were supplemented with fixed amounts of Mg^{2+} to yield samples with Mg^{2+} concentrations varying from 0.01 to 0.20 mM Mg^{2+} . For the fluorescence experiments, Mg^{2+} was added in a 1.1:1 ratio in order to have a slight excess of Mg^{2+} , while furaptra was added at a concentration of 2 μ M. For the G_t release experiments, 1.0 mM Mg^{2+} was added to allow G_t to function, since Mg^{2+} is required for the proper functioning of all G-proteins, including G_t [5,21].

After Mg^{2+} readdition, these reconstituted G_t samples (G_t samples that had Mg^{2+} removed and then re-added) were then titrated with Li^+ concentrations ranging from 0 to 30 mM for the NMR experiments or from 0 to 50 mM Li^+ for the fluorescence and G_t release experiments. The NMR and fluorescence experiments that involved SROS membranes with or without bound G_t were conducted in the dark under a dim red light to avoid photobleaching of the ROS membranes.

2.4. G_t release from SROS membranes

The effect of Li^+ on G_t release from SROS membranes was determined using a modification of a procedure described in the literature [15]. Briefly, SROS membranes were first photobleached under normal room light for 1 min on ice. Photobleaching of the rhodopsin in the SROS membranes must be done on ice to prevent their overbleaching, since overbleached rhodopsin slowly decays into metarhodopsin III, retinal and opsin, all of which are known to bind G_t poorly [25]. These photobleached membranes now contain R^* , which readily binds G_t [26].

In order to confirm that the removal of the bound Mg^{2+} from G_t did not denature the protein, the results from our experiments using reconstituted G_t were compared with the results from previous experiments in which native G_t (protein that did not have its bound Mg^{2+} removed) was used [15]. The G_t release values that we obtained from our experiments with 2 mM Mg^{2+} but no Li^+ (57.2%) agreed well with those G_t release values in which native G_t in the presence of 2 mM Mg^{2+} was used (55%) [15]. For these control experiments, an excess of Mg^{2+} (2 mM) was used [15], but our experiments determined that only 1 mM Mg^{2+} is actually needed to give comparable G_t release values. This is the reason why only 1 mM Mg^{2+} was readded to reconstitute our G_t samples. Thus, these experiments with native G_t

provided a control with which to compare the results from our G_t release experiments to see if Li^+ would affect the release of G_t from SROS membranes. Therefore, our modified protocol called for mixing of 25 μ M of photobleached SROS membranes were then mixed with 5 μ M of reconstituted G_t (apo G_t with 1 mM Mg^{2+} readded to it) in a buffer containing 10 mM 3-[N-morpholino] propanesulphonic acid (MOPS; pH 7.5), 2 mM DTT and varying concentrations of either Li^+ (15, 30 or 50 mM), K^+ (15 or 30 mM), or Mg^{2+} (1 mM).

This SROS/ G_t mixture was then allowed to incubate for 20 min in the dark. Dark conditions must be used to prevent overbleaching of rhodopsin in the SROS membranes and to facilitate G_t binding to rhodopsin in the SROS membranes. To these tubes, 1 μ M of a non-hydrolyzable analog of GTP, β, γ -imidoguanosine 5'-triphosphate (Gpp(NH)p), was then added. After a 5 min incubation period with Gpp(NH)p, the G_t in solution was separated from the membrane-bound G_t by centrifugation at 20 psi for 5 min in a Beckman Airfuge. The supernatants were analyzed for protein content by UV analysis, as described above [22].

2.5. Nuclear magnetic resonance spectrometry

The NMR experiments were conducted on a Varian VXR-300 NMR spectrometer using a 10 mm broadband probe. All samples were run at room temperature with spinning at 16–18 Hz. 7Li NMR spectra were recorded at 116.5 MHz with a spectral width of 10,000 Hz and an acquisition time of 0.979 s. 7Li T_1 relaxation measurements were determined using the inversion recovery pulse sequence ($D_1-180^\circ-\tau-90^\circ$). At least seven τ values were used for each spin–lattice relaxation time (T_1) determination, and an interpulse delay of at least 5 times the T_1 value was used before repeating the pulse sequence. The relaxation measurements were often accompanied by a 10% uncertainty. The reported apparent Li^+ binding constants, K_{app} , are the averages from two separately prepared samples with error bars that represent the range of the calculated values.

2.5.1. Calculation of Li^+ and Mg^{2+} binding constants from 7Li NMR T_1 measurements to G_t , SROS and ROS-T

The K_{app} values were calculated from James–Noggle plots according to Eq. (1) using at least five 7Li T_1 values [27,28]. The calculation of K_{app} from 7Li T_1 measurements assumes a two-state (free, f, and bound, b, metal ions) model undergoing fast exchange that uses a total binding site concentration, [B], and thus, $[Li^+]_t \sim [Li^+]_f$ [27–31]:

$$\begin{aligned} \Delta R^{-1} &= (R_{obs} - R_f)^{-1} \\ &= K_{app}^{-1} \{ [B] (R_b - R_f) \}^{-1} + [Li^+]_t \{ [B] (R_b - R_f) \}^{-1}, \end{aligned} \quad (1)$$

where all symbols are defined as in the abbreviations, respectively. K_{app} can be calculated from Eq. (1) using the quotient of the slope by the y -intercept and then multiplying by 1000, which yields K_{app} values in M^{-1} .

From this competition model, even assuming a single binding site or a number of equivalent independent binding sites for Li^+ and Mg^{2+} , the true Li^+ and Mg^{2+} binding constants for G_t and the other systems cannot be directly determined from the experimental data when both ions are present because Li^+ displaces Mg^{2+} and vice versa. Thus, in the presence of Mg^{2+} , only an apparent Li^+ binding constant can be directly determined from the experimental data. However, the true Li^+ and Mg^{2+} binding constants can be determined by plotting K_{app}^{-1} vs. $[Mg^{2+}]_t$ using the following equation [30]:

$$K_{app}^{-1} = K_{Li}^{-1} (1 + K_{Mg} [Mg^{2+}]_f), \quad (2)$$

where K_{Li} is the Li^+ binding constant in the absence of other metal ions (the true Li^+ binding constant), K_{Mg} is the Mg^{2+} binding constant in the absence of other metal ions (the true Mg^{2+} binding constant) and $[Mg^{2+}]_f$ (assumed $\sim [Mg^{2+}]_t$) is the free Mg^{2+} concentration.

2.6. Fluorescence spectroscopy

Fluorescence experiments were conducted using a Photon Technology International QuantaMaster QM-1 fluorimeter. Fluorescence data was recorded using furaptra, by scanning the excitation spectrum from 300 to 400 nm while monitoring the emission at 510 nm [32–34]. Fluorescence experiments using purified G_t alone were conducted at room temperature, while the fluorescence experiments using SROS membranes with and without bound G_t were conducted at 4 $^\circ$ C to increase the stability of the SROS. The effect of the temperature difference of the K_{app} values was corrected using the Van't Hoff equation. For those fluorescence experiments conducted at 4 $^\circ$ C, a cooling unit was connected to the fluorimeter.

2.6.1. Calculation of $[Mg^{2+}]_f$ values from fluorescence spectroscopy data

When using furaptra, the free Mg^{2+} concentration, which was corrected for Li^+ binding to furaptra [26,32], was calculated from the following equation:

$$\begin{aligned} [Mg^{2+}]_f &= \frac{K_d S_{min} (R - R_{min})}{S_{max} (R_{max} - R)} \\ &+ \frac{K_d S'_{max} (R - R'_{max}) [Li^+]_f}{K'_d S_{max} (R_{max} - R)}, \end{aligned} \quad (3)$$

where R , R_{min} , R_{max} , R'_{max} , S_{min} , S_{max} , S'_{max} , K_d and K'_d are defined in the abbreviations footnote.¹ The second term of the equation compensates for the weak interaction between the dye and Li^+ . As a large excess of Li^+ is used in this experiment, then $[Li^+]_t \sim [Li^+]_f$.

The K_d values for Mg^{2+} and Li^+ to furaptra at room temperature were previously reported to be 1.50 and 250 mM, respectively [29,32,34]. We measured the K_d values of Mg^{2+} and Li^+ to furaptra at 4 °C and found them to be 4.12 and 530 mM, respectively [35].

2.7. Statistical analysis

The statistical significance of differences between sets of data was assessed using a paired Student's *t*-test.

3. Results

3.1. Competition between Li^+ and Mg^{2+} for the Mg^{2+} binding sites on SROS membrane with and without G_t , and with G_t alone using 7Li NMR

Fig. 1(a) and (c) illustrate that the linear increase in 7Li T_1 values with increasing Li^+ concentration for those systems containing G_t was more pronounced in the presence of 0.05 mM Mg^{2+} than in its absence. In fact, the slopes of such linear correlations for ROS-T and G_t alone are significantly larger ($p < 0.01$) in the presence of Mg^{2+} (0.46 and 0.28, respectively) than in its absence (0.34 and 0.10, respectively). Fig. 1(b), however, illustrates that the increase in the 7Li T_1 values for SROS was not greatly affected by the addition of 0.05 mM Mg^{2+} . The slope for the SROS correlation in the presence of Mg^{2+} (0.39) is not significantly different ($p > 0.05$) from the value in the absence of Mg^{2+} (0.35).

Using these 7Li T_1 measurements, James–Noggle plots were constructed [27,28] to calculate the K_{app} values for Li^+ binding to ROS-T, SROS and for G_t alone in the presence of increasing amounts of Mg^{2+} (0.01–0.2 mM). The Li^+ K_{app} values for ROS-T were the largest for all systems at very low concentrations of added Mg^{2+} and also showed the largest decrease with increasing $[Mg^{2+}]_t$ (480 ± 18 – 98 ± 15 M^{-1}), while the K_{app} values for SROS showed a much smaller decrease under similar conditions (270 ± 29 – 130 ± 4 M^{-1}). The magnitude of the decrease in the K_{app} values for G_t alone, however, was in between (235 ± 3 – 60 ± 2 M^{-1}) those for ROS-T and for SROS. Thus, the Li^+ K_{app} values for ROS-T are the largest in the absence of Mg^{2+} and the most sensitive of the three systems to increasing Mg^{2+} concentrations.

Plots of K_{app} vs. $[Mg^{2+}]_t$ also show that the binding strength of both ROS-T and G_t to Li^+ exhibits a biphasic dependence on $[Mg^{2+}]_t$. The initial points for the graphs of ROS-T and G_t at low Mg^{2+} concentrations (0.01–0.1 mM) produce straight lines with much larger slopes (–2500 and –1340, respectively) than the slopes (–1320 and –446, respectively) for those points at higher Mg^{2+} concentrations (0.1–0.2 mM). Both graphs seem to have a break point around 0.08 mM Mg^{2+} . On the

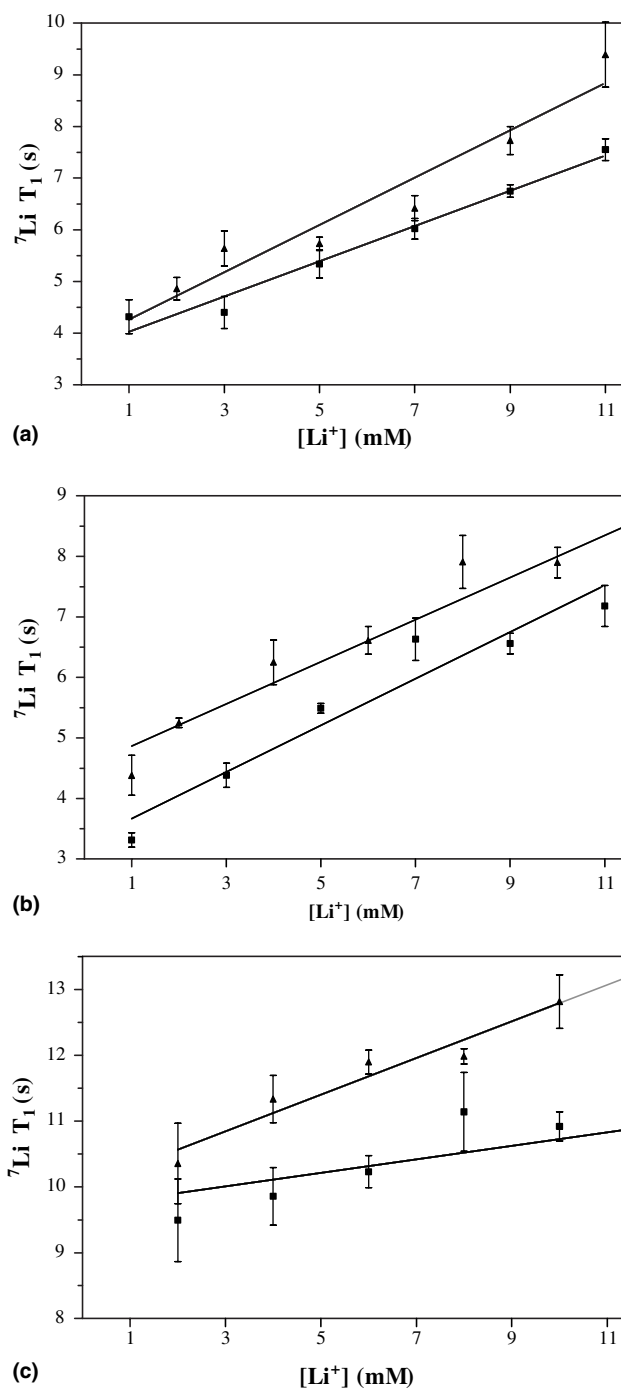


Fig. 1. 7Li T_1 measurements for bovine SROS membranes with (a) and without (b) heterotrimeric G_t and for G_t alone (c) in the absence (■) or the presence (▲) of 0.05 mM Mg^{2+} . The SROS membrane protein concentration was 9.0 ± 0.8 mg/ml and all experiments were conducted at 20 ± 1 °C in a 10 mm NMR probe in a dark room under a dim red light. The error bars denote the range of values obtained from two different trials.

other hand, the corresponding dependence of K_{app} on $[Mg^{2+}]_t$ for SROS is linear.

Fig. 2 is a graphical representation of Eq. (2), where the data is plotted as K_{app}^{-1} vs. $[Mg^{2+}]_t$. According to Eq. (2), if all binding sites are independent, equivalent, and if

$[Mg^{2+}]_t \sim [Mg^{2+}]_f$, the curves should be linear with intercepts and slopes equal to K_{Li}^{-1} and (K_{Mg}/K_{Li}) , respectively, where K_{Li} and K_{Mg} are the true Li^+ and Mg^{2+} binding constants. The curve for SROS in Fig. 2 is linear ($R^2 = 0.999$), indicating that a single type of equivalent Li^+ and Mg^{2+} binding site is indeed present for SROS. The binding of both ions to SROS is weak, as shown by the fact that $[Mg^{2+}]_t \sim [Mg^{2+}]_f$ holds even at very low $[Mg^{2+}]_t$, and by the estimated values K_{Li} and K_{Mg} (310 ± 17 and $6760 \pm 405 M^{-1}$, respectively), which were obtained from Eq. (2) by extrapolating the SROS data from Fig. 2. However, the graphs for both G_t and ROS-T are not linear, reflecting the presence of more than one type of ion binding sites. The graph for G_t is clearly biphasic, with a break point around 0.08 mM Mg^{2+} , where the two linear sections of the plot are each defined by four different K_{app}^{-1} values ($R^2 = 0.998$ for $[Mg^{2+}]_t < 0.08$ mM and $R^2 = 0.993$ for $[Mg^{2+}]_t > 0.08$ mM). Assuming that $[Mg^{2+}]_t \sim [Mg^{2+}]_f$, the K_{Li} and K_{Mg} values for G_t at low $[Mg^{2+}]_t$ were estimated to be 260 ± 6 and $12,400 \pm 400 M^{-1}$, respectively, while at high $[Mg^{2+}]_t$, K_{Li} and K_{Mg} were 332 ± 44 and $22,530 \pm 1,800 M^{-1}$, respectively. However, these estimates should have only qualitative value, as the assumption that $[Mg^{2+}]_t \sim [Mg^{2+}]_f$ probably does not apply, particularly when $[Mg^{2+}]_t < 0.1$ mM since the total G_t concentration is 0.1 mM. The graph for ROS-T in Fig. 2 is neither linear nor biphasic, as the three points above 0.08 mM $[Mg^{2+}]_t$ give a low $R^2 = 0.961$, reflecting the presence of several types of ion binding sites.

The above calculations of the Li^+ and Mg^{2+} binding constants from Eq. (2) are based on very accurate protein concentrations only for G_t , because the purity and

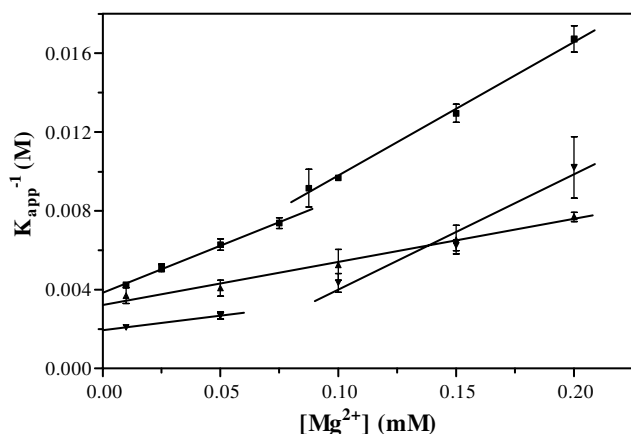


Fig. 2. Variation of values of K_{app}^{-1} with $[Mg^{2+}]_t$ for SROS membranes with (\blacktriangledown) and without (\blacktriangle) heterotrimeric G_t , using the same dark experimental conditions as for Fig. 1(a), and for purified G_t alone (\blacksquare), in the presence of varying concentrations of $MgCl_2$. The SROS membrane protein concentration was 9.0 ± 0.8 mg/ml. The concentration of purified G_t used was 0.1 mM. The concentration range of $LiCl$ varied from 1–30 mM. The reported, apparent Li^+ binding K_{app} values are the averages from 2 separately prepared samples. The error bars represent the range of the values obtained.

concentration of the SROS and ROS-T systems could not be determined consistently and accurately. The concentration of G_t bound to the SROS membrane in the ROS-T system is not constant as a result of the procedure for sample preparation. The SROS system could also possibly have different concentrations of neutral and negatively-charged phospholipids, which would affect the calculated Li^+ and Mg^{2+} binding constants.

3.2. Competition between Li^+ and Mg^{2+} for the Mg^{2+} binding sites on SROS membranes in the absence and presence of G_t and in purified G_t alone using fluorescence spectroscopy

Fluorescence measurements using furaptra were conducted on ROS-T and SROS membranes. Fig. 3 shows the fluorescence excitation spectra of a solution of ROS-T membrane containing 2 μM furaptra, 2.2 mM $MgCl_2$ and 150 mM Tris-Cl (pH 7.4) that were titrated with various Li^+ concentrations. An increase in $[Li^+]$ resulted in a blue-shift of the fluorescence spectrum (Fig. 3). Table 1 shows the calculated $[Mg^{2+}]_f$ values (after correction for Li^+ binding to furaptra) of solutions of ROS-T and SROS membranes that were titrated with Li^+ [29,35]. Comparison of the calculated $[Mg^{2+}]_f$ values for both ROS-T and SROS membranes shows that the values obtained from ROS-T membranes are significantly lower than those obtained from SROS membranes. In the absence of Li^+ , 67% of the Mg^{2+} in the SROS membrane sample is free, compared to 45% of the Mg^{2+} being free in the ROS-T membrane sample (Table 1). Upon addition of 50 mM Li^+ , nearly 100% of the Mg^{2+} is free in the SROS membrane sample, compared to 65% of the Mg^{2+} being free in the ROS-T membrane sample

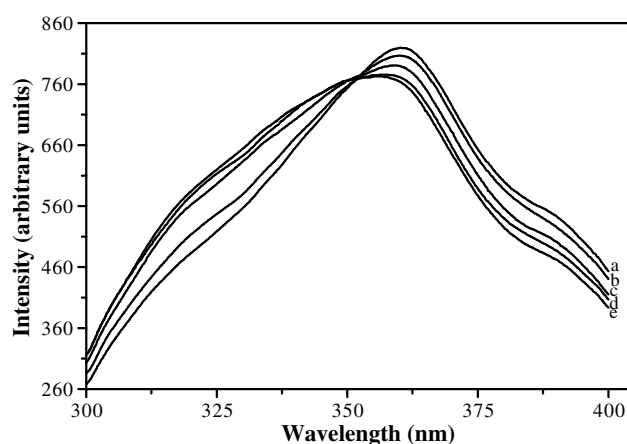


Fig. 3. Fluorescence excitation spectra of 2 μM furaptra in a solution containing G_t -bound SROS membrane, 2.2 mM $MgCl_2$ and 150 mM Tris-Cl, pH 7.4, and (a) 0 mM $LiCl$, (b) 5 mM $LiCl$, (c) 10 mM $LiCl$, (d) 20 mM $LiCl$ and (e) 50 mM $LiCl$. The membrane protein concentration was 1.04 mg/ml.

Table 1

Fluorescence-determined $[Mg^{2+}]_f$ values for ROS membrane suspensions with and without G_t ^a

$[Li^+]/mM$	SROS membranes ^b		ROS-T membranes ^c		Ratio of Mg^{2+} release from SROS over ROS-T ($[Mg^{2+}]_{f,SROS}/[Mg^{2+}]_{f,ROS-T}$)
	R^d	$[Mg^{2+}]_f$ (mM)	R^d	$[Mg^{2+}]_f$ (mM)	
0	1.06	1.48	0.94	1.00	1.49
5	1.12	1.73	0.99	1.20	1.44
10	1.18	1.99	1.04	1.37	1.46
50	1.27	2.20	1.11	1.44	1.53

^a The reported values represent an average of measurements conducted in three separately prepared samples. All samples contained 2 μM furaptra, 2.2 mM $MgCl_2$, and 0.15 M Tris-Cl, pH 7.4, at 4 °C.

^b The total protein concentration was 0.85 mg/ml.

^c The total protein concentration was 1.04 mg/ml.

^d The errors in the determination of the R values (F_{335}/F_{370}) were less than 10%.

(Table 1). The protein concentration was a factor of 1.22 in the ROS-T membrane samples as compared to the SROS membrane samples, but the $[Mg^{2+}]_f$ values were decreased by a factor of 1.53 ± 0.10 (Table 1, last column). This unexpected result, which indicates that the presence of G_t in the ROS membrane (ROS-T) decreases the displacement of bound Mg^{2+} upon addition of Li^+ , led us to investigate the effect of G_t on Mg^{2+} binding and displacement in the presence of Li^+ .

Fluorescence experiments, using furaptra, were conducted with purified G_t in its inactive GDP-bound conformation. Fig. 4 shows the fluorescence spectra obtained when a solution, containing 100 μM G_t , 100 μM GDP and 300 μM Mg^{2+} , was titrated with Li^+ . Again, as the Li^+ concentration increased, the spectrum of the Mg^{2+} -sensitive dye was blue shifted. Table 2 shows the calculated $[Mg^{2+}]_f$ values (after correction for Li^+ binding to furaptra) for the solution of the GDP-bound form of G_t after titration with Li^+ [29,35]. This table also indicates that there are, at least, three Mg^{2+} binding sites per G_t molecule, since 300 μM Mg^{2+} is completely bound to 100 μM G_t .

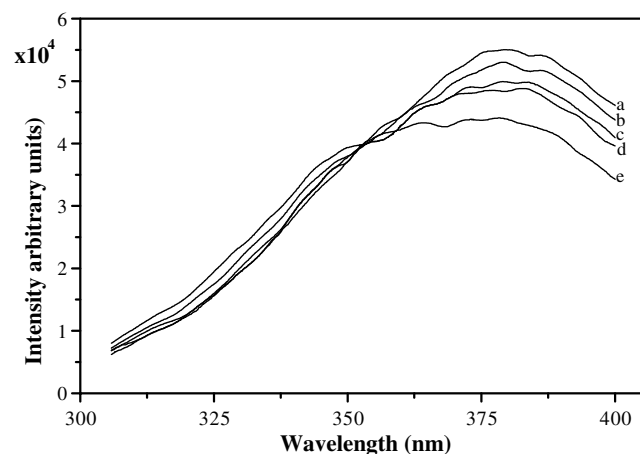


Fig. 4. Fluorescence excitation spectra of 100 μM G_t and 100 μM GDP with 300 μM Mg^{2+} alone (a), and titrated with Li^+ (Traces b through e). The Li^+ concentrations were: (b) 5 mM, (c) 10 mM, (d) 20 mM, and (e) 50 mM.

3.3. Effect of Li^+ on the release of G_t bound to SROS membranes

The amount of G_t released from the SROS membranes was affected by the addition of Li^+ (Table 3). The amount of G_t released from the SROS membranes decreased from 57.2% for the control experiment, which contained 1 mM Mg^{2+} , to 45.4%, 47.4%, and 41.5%, after the addition of 15, 30 and 50 mM Li^+ , respectively. This decrease in the amount of released G_t from the SROS membranes was found to be statistically significant.

Table 2

Fluorescence-determined $[Mg^{2+}]_f$ values for G_t solutions titrated with Li^+ ^a

$[Li^+]$ (mM)	R^b	$[Mg^{2+}]_f$ (μM)
0	0.48	0
5	0.54	87
10	0.58	137
20	0.63	178
50	0.72	195

^a The reported values represent an average of measurements conducted in three separately prepared samples. All samples contained 2 μM furaptra, 100 μM G_t , 100 μM GDP, 300 μM $MgCl_2$, and 0.15 M Tris-Cl, pH 7.4, at 25 °C.

^b The errors in the determination of the R values (F_{335}/F_{370}) were less than 10%.

Table 3

Effect of Li^+ and K^+ on the release of G_t from SROS membranes^a

Cation	$[G_t]_{added}$ (μM)	$[G_t]_{released}$ (μM)	Protein released (%)
1 mM Mg^{2+}	4.95	2.83 ± 0.09	57.2 ± 1.76
15 mM Li^+	4.95	2.25 ± 0.30	45.4 ± 4.98
30 mM Li^+	4.95	2.35 ± 0.15	47.4 ± 3.03
50 mM Li^+	4.95	2.05 ± 0.13	41.5 ± 2.60
15 mM K^+	4.95	2.78 ± 0.18	56.1 ± 3.66
30 mM K^+	4.95	2.70 ± 0.08	54.6 ± 1.53

^a The reported values represent an average of measurements conducted in three separately prepared samples.

^b All G_t samples were prepared in a 10 mM MOPS (pH 7.5) buffer containing 2 mM DTT and 1 mM Mg^{2+} before the addition of one of the above cation concentrations.

cant ($p < 0.05$). In contrast, the addition of 15 or 30 mM K^+ did not result in a statistically significant ($p > 0.05$) decrease in the amount of released G_t (Table 3), as compared to the control condition.

4. Discussion

It is known that G-proteins require Mg^{2+} to function [4,5]. Specifically, Mg^{2+} ions must bind to a high affinity (K_d in nM) Mg^{2+} binding site for the G-protein to possess its GTPase activity and to a low affinity (K_d in mM) Mg^{2+} binding site for the G-protein to possess its GDP/GTP exchange activity [5,14]. Because Li^+ and Mg^{2+} ions have similar chemical and physical properties [1,13], competition between Li^+ and Mg^{2+} for the Mg^{2+} binding sites in G-proteins is plausible. We have previously demonstrated Li^+ and Mg^{2+} competition for Mg^{2+} binding sites in intact cells and various biomolecules [29,35–40]. Evidence of Li^+ and Mg^{2+} competition for the Mg^{2+} binding site(s) of various Mg^{2+} -dependent enzymes [41,42], including G-proteins [8,9,13,14] has also been reported. In this study, we used 7Li T_1 relaxation measurements and fluorescence spectroscopy with the Mg^{2+} fluorophore, furaptra, to examine the Li^+/Mg^{2+} competition hypothesis in three model systems: the purified G-protein G_t , stripped ROS membranes with bound G_t (ROS-T), and stripped ROS membranes without bound G_t (SROS).

Since the observed 7Li T_1 values are a weighted average of the free and bound 7Li T_1 values, they represent a function of free Li^+ concentrations and, indirectly, a function of free Mg^{2+} concentrations [27,35,43], because Li^+ and Mg^{2+} compete for the same Mg^{2+} binding sites. Therefore, this method is sensitive to both Li^+ -induced Mg^{2+} displacement and Mg^{2+} -induced Li^+ displacement. The 7Li T_1 values obtained for ROS-T, SROS and G_t alone, in the absence and presence of 0.05 mM Mg^{2+} increase linearly as $[Li^+]$ increases, and this indicates that Li^+ binds to both membrane systems and to G_t itself (Fig. 1(a)–(c), respectively). The addition of Mg^{2+} resulted in large increases in the slopes of the corresponding curves for ROS-T membrane and G_t , whereas the slope remained constant for the SROS membrane curve, demonstrating that the presence of G_t decreases the binding of Li^+ , as Li^+ competes to a lesser extent for the binding sites occupied by Mg^{2+} .

When both ROS-T and SROS membrane samples were titrated with Li^+ in the presence of increasing amounts of Mg^{2+} , the K_{app} values for Li^+ binding decreased due to Mg^{2+} -induced Li^+ displacement. The increase of K_{app}^{-1} with $[Mg^{2+}]_t$ (Fig. 2), plotted according to Eq. (2), is linear for SROS membranes, reflecting the presence of a single type of relatively weak, equivalent Li^+ and Mg^{2+} binding sites with constant K_{Li} and K_{Mg} values, and $K_{Mg}/K_{Li} \sim 22$, leading to $[Mg^{2+}]_f \sim [Mg^{2+}]_t$.

However, the behaviour of K_{app} for Li^+ binding to ROS-T was more complicated: at low $[Mg^{2+}]$ (<0.1 mM), Mg^{2+} is able to displace large amounts of Li^+ , reflected in the large decrease in the Li^+ K_{app} values, while at larger $[Mg^{2+}]$ (≥ 0.1 mM), a much smaller amount of Li^+ is displaced, again reflected in the smaller decrease in the Li^+ K_{app} values at larger Mg^{2+} concentrations. Consequently, the curve for ROS-T in Fig. 2 is not linear, reflecting Li^+/Mg^{2+} competition at more than one type of ion binding sites with different affinities for both ions. In order to determine whether this non-linear pattern was caused by G_t itself or by its interaction with the SROS membranes, 7Li T_1 relaxation measurements were conducted on G_t alone.

The plot of K_{app}^{-1} vs. $[Mg^{2+}]_t$ (Fig. 2), generated on the basis of the 7Li T_1 measurements when samples of purified G_t were titrated with Li^+ in the presence of increasing amounts of Mg^{2+} , is clearly biphasic, with a break point around 0.08 mM Mg^{2+} . At lower $[Mg^{2+}]_t$ (<0.08 mM), Mg^{2+} was able to displace larger amounts of Li^+ than at higher $[Mg^{2+}]_t$ (>0.08 mM). This again suggests Li^+/Mg^{2+} competition for two types of cation binding sites in G_t with different affinities for both ions.

Thus, Fig. 2 demonstrates the biphasic nature of the competition between Li^+ and Mg^{2+} in the G_t samples, while for ROS-T the competition model seems to be more complex. At a concentration as low as 0.025 mM Mg^{2+} , Mg^{2+} addition decreased the K_{app} values for Li^+ binding by $100 M^{-1}$ for ROS-T and by $40 M^{-1}$ for G_t , indicating that a small amount of Mg^{2+} is able to displace a large amount of Li^+ , presumably from the high-affinity Mg^{2+} binding site. Since the competitive Li^+ concentrations were two to three orders of magnitude higher than those of Mg^{2+} , the affinity of Li^+ for the high-affinity Mg^{2+} binding site must be rather low. Thus, it is likely that at physiological Mg^{2+} concentrations, Li^+ modulates Mg^{2+} binding in a competitive manner primarily by competing for the low affinity Mg^{2+} binding sites.

Fig. 2 also shows that the binding site(s) available to Li^+ are stronger for ROS-T than for SROS and G_t , suggesting that the G_t -ROS membrane interface increases the affinity of the G_t low affinity metal binding sites for Li^+ binding. The presence of these binding sites may be the source of the higher complexity of the ion competition observed for ROS-T relative to SROS and G_t . However, the dependence of Li^+ binding K_{app} values to ROS-T on Mg^{2+} concentration did not fit this simple model.

Our NMR studies demonstrated Li^+ binding to ROS-T and G_t and Li^+ -induced displacement of Mg^{2+} are also from these two systems. The fluorescence spectra provided evidence for a Li^+ concentration-dependent release of Mg^{2+} from ROS-T and from G_t (Figs. 3 and 4). As the Li^+ concentration was increased, the fluorescence spectra of ROS-T and of G_t -containing sam-

ples were blue shifted, indicating displacement of Mg^{2+} by Li^+ in both systems. Thus, as with the NMR results for these two systems, the fluorescence spectra (Figs. 3 and 4) support the conclusion that Li^+ addition causes Mg^{2+} displacement from these two systems.

Other fluorescence experiments demonstrate that Mg^{2+} is displaced more effectively from the SROS than from ROS-T (Table 1). With G_t addition, the total protein concentration in the ROS-T system was increased by a factor of 1.22 over the SROS system, which would be expected to result in an increase in the number of Mg^{2+} binding sites and a decrease in $[Mg^{2+}]_f$ in G_t and in particular for ROS-T, where competition leads to a more pronounced break in the graph. However, $[Mg^{2+}]_f$ decreased by a larger factor of 1.53 ± 0.10 (Table 2, last column). Thus, the decreased $[Mg^{2+}]_f$ in the ROS-T samples as compared to the SROS samples cannot solely be attributed to the increase in protein concentration of the ROS-T system. It may be due to the presence of high affinity Mg^{2+} binding sites on the bound G_t in the ROS-T system.

Table 2 indicates that there are three Mg^{2+} binding sites per G_t molecule. It also shows that even at 50 mM Li^+ , only two thirds of the Mg^{2+} initially present is displaced from G_t . However, as Table 1 indicates, at 50 mM Li^+ all the Mg^{2+} is displaced from the SROS. These results indicate the presence in the G_t molecule of one Mg^{2+} binding site that selectively binds Mg^{2+} even in the presence of large amounts of Li^+ . This high affinity Mg^{2+} binding site is responsible for the biphasic response of the plots of K_{app}^{-1} vs. $[Mg^{2+}]$ for G_t and ROS-T (Fig. 2). However, even at 5 mM Li^+ , a small amount of Mg^{2+} is displaced from G_t (Table 2), suggesting the presence of two low affinity Mg^{2+} binding sites from which Li^+ can effectively displace Mg^{2+} even in the presence of excess Mg^{2+} . Thus, the fluorescence data indicate Li^+ displacement of Mg^{2+} from G_t and suggest that there are two types of Mg^{2+} binding sites on G_t that have different affinities for Mg^{2+} . The Li^+ displacement of Mg^{2+} occurs only at the low affinity Mg^{2+} binding sites.

However, the purpose of this study was not the full characterization of these two types of Mg^{2+} binding sites. The affinities of these two types of Mg^{2+} binding sites both for Li^+ and Mg^{2+} along with their location will be the focus of a future study in which this Li^+/Mg^{2+} competition hypothesis will also be tested in the GTP bound form of G_t .

The biophysical studies described above provide evidence for an ionic competition mechanism between Li^+ and Mg^{2+} for the Mg^{2+} binding sites on G_t , where Li^+ can displace Mg^{2+} at the low affinity Mg^{2+} -binding sites of the protein, in accordance with the hypothesis [8,14] previously proposed for the G-proteins present in the membranes from rat cerebral cortex. Li^+ binding to G_t may affect its functional properties such as its release

from the SROS membranes. The ability of Li^+ to regulate G_t release may be important for the understanding of its pharmacological action in the treatment of bipolar disorder. Thus, the effect of Li^+ on G_t release from SROS membranes was examined.

At concentrations of 15, 30 and 50 mM, Li^+ was found to inhibit the release of G_t from SROS membranes in the presence of Gpp(NH)p (Table 3). At 15 mM, the amount of released G_t was significantly decreased ($p < 0.05$) by 17%, in comparison to the control condition, while, at 50 mM Li^+ , the amount of released G_t was significantly decreased ($p < 0.05$) by 27%, as compared to the control condition. To ensure that this effect was not due to ionic strength, G_t release experiments were also conducted in 15 and 30 mM K^+ . At these two K^+ concentrations, the amount of released G_t was not statistically different ($p > 0.05$) from the control experiment (Table 3). Thus, this effect was not due to ionic strength. Therefore, Li^+ is able to inhibit G_t release, probably by displacing Mg^{2+} , presumably from the low affinity Mg^{2+} binding sites, which are known to be necessary for the release of G_t from the SROS membranes [5,14]. By decreasing the amount of released G_t , Li^+ can alter the signal transducing properties of this G-protein, ultimately inhibiting the G-protein's ability to produce an intracellular effect in response to an extracellular signal.

In summary, the multinuclear NMR methods developed by us and others for small molecules to probe Li^+ binding as well as Li^+/Mg^{2+} competition [29,35–40,44,45] were extended to the 84.5 kDa G-protein G_t . Using these NMR methods based on 7Li T_1 relaxation measurements, and fluorescence spectroscopy with the Mg^{2+} fluorophore, furtrapra, we have demonstrated that Li^+ binds to G_t , ROS-T and SROS and that Li^+ competes with Mg^{2+} in a biphasic manner for G_t and ROS-T, suggesting two types of Mg^{2+} binding sites of different affinity. Additionally, in the present study, we demonstrated that Li^+ is able to inhibit the release of G_t from SROS membranes, presumably by displacing Mg^{2+} from the low affinity Mg^{2+} binding sites. By inhibiting the release of G_t from SROS membranes, Li^+ may be able to modulate the activity of G_t .

Considering the homology of the high-affinity Mg^{2+} binding site among all G-proteins [16–21], and the present study, it is unlikely that Li^+/Mg^{2+} competition can occur at this site. By contrast, sequence and structural analyses of the low-affinity Mg^{2+} binding site are unavailable. Further characterization of these two types of Mg^{2+} binding sites in transduction in other conformations as well as in other G-proteins will be attempted in future studies to determine whether Li^+ may be able to compete for the low-affinity Mg^{2+} site and modulate the activity of G-proteins, which ultimately, may be one of the mechanisms of lithium action in the treatment of bipolar disorder.

The therapeutic 0.5–1.0 mM concentration range of Li^+ corresponds to plasma concentrations, but, as our recent studies with different types of cells show [46], Li^+ can concentrate intracellularly up to approximately 3–5 mmol/l cells, which corresponds to 5–8 mM (assuming that the cytoplasmatic volume is roughly 80% of the cell volume). Because the G protein targets are intracellular, we predict that at therapeutic intracellular Li^+ concentrations, Li^+ competes with ~20–30% Mg^{2+} and is responsible for ~10% of Li^+ -induced $\text{G}_{\text{t}\alpha}$ release. However, high concentrations of Mg^{2+} (5–100 mM) are found to increase the rate of binding of $\text{GTP}\gamma\text{S}$ to both G_s and G_i and consequently their rate of activation by $\text{GTP}\gamma\text{S}$, indicating that low affinity Mg^{2+} site(s) are involved here. This process requires removal of GDP first from the G_α site. GDP dissociates slowly from isolated G_α , but binds almost irreversibly to $\text{G}_{\alpha\beta\gamma}$, thereby rendering activation dependent on G_α interaction with hormone-activated membrane receptors. The GDP binding and dissociation from isolated G_α . GDP depends on the structure and flexibility/rigidity of the switch I (G2 loop) and switch II (G3 loop and $\alpha 2$) regions, which are disordered in this form. Thus, a low affinity Mg^{2+} ion would probably bind close to these regions, whose conformations are directly affected by $\text{G}_{\beta\gamma}$ binding and indirectly by receptor interactions. Li^+ competition with the low-affinity Mg^{2+} site would antagonize the mM range effects of Mg^{2+} , but not the μM range effects. This means that Li^+ would retard the processes leading to G_α activation, but would not affect the deactivation GTP hydrolysis process.

5. Abbreviations

cAMP	cyclic adenosine 3', 5'-monophosphate
DAG	diacylglycerol
DTT	dithiothreitol
EDTA	ethylenediamine- <i>N,N,N',N'</i> -tetraacetic acid
G-protein	guanine nucleotide-binding protein
G_t	transducin
$\text{G}_{\text{t}\alpha}$, $\text{G}_{\text{t}\beta}$, and $\text{G}_{\text{t}\gamma}$	α , β , and γ subunits of transducin
GDP	guanosine-5'-diphosphate
Gpp(NH)p	β , γ -imidoguanosine 5'-triphosphate
GTP	guanosine-5'-triphosphate
ICP-ES	inductively coupled plasma emission spectrometry
IP_3	inositol 1,4,5-triphosphate
$[\text{Li}^+]_f$	concentration of free Li^+ ions
$[\text{Li}^+]_t$	total concentration of Li^+ ions
K_{app}	apparent Li^+ binding constant
K_d	dissociation constant
K_{Li}	Li^+ binding constant

K_{Mg}	Mg^{2+} binding constant
$[\text{Mg}^{2+}]_f$	concentration of free Mg^{2+} ions
$[\text{Mg}^{2+}]_t$	total concentration of Mg^{2+} ions
MOPS	3-[N-morpholino]propanesulphonic acid
PI	phosphatidyl inositol
PDE	phosphodiesterase
PMSF	phenylmethylsulphonyl fluoride
Psi	pounds per square inch
R^*	photoexcited rhodopsin
R_b	the reciprocal of the T_{1b}
R_f	the reciprocal of the T_{1f}
R_{max} and R'_{max}	intensity ratios in the presence of saturating amounts of Mg^{2+} or Li^+ , respectively
R_{min}	intensity ratio in the absence of metal ions
R_{obs}	the reciprocal of the $T_{1\text{obs}}$
RBCs	red blood cells
ROS	rod outer segment
ROS-T	stripped ROS membranes reattached to G_t
S_{max} and S'_{max}	fluorescence intensities at 510 nm after excitation at 370 nm in the presence of saturating amounts of Mg^{2+} or Li^+ , respectively
S_{min}	fluorescence intensity at 510 nm after excitation at 370 nm in the absence of metal ions
SROS	stripped ROS membranes without bound transducin
T_1	spin-lattice relaxation time
T_{1b}	the T_1 value in the presence of saturating amounts of substrate
T_{1f}	the T_1 value in the presence of saturating amounts of Li^+
$T_{1\text{obs}}$	the experimentally-determined T_1 value
Tris	Tris[hydroxymethyl]aminomethane

Acknowledgements

Financial support from NIMH (grant number MH-45926) is acknowledged by D.M. de F., and from Fundação da Ciência e Tecnologia (FCT), Portugal (grant POCTI/1999/BCI/36160) by C.F.G.C.G.

References

- [1] N.J. Birch, Chem. Rev. 99 (1999) 2659–2682.
- [2] R.H. Lenox, R.K. McNamara, R.L. Papke, H.K. Manji, J. Clin. Psychiatry 59 (1998) 37–47.
- [3] R.S. Jope, Mol. Psychiatry 4 (1999) 117–128.
- [4] H.E. Hamm, J. Biol. Chem. 273 (1999) 669–672.
- [5] A.G. Gilman, Ann. Rev. Biochem. 56 (1987) 615–649.

- [6] G. Schreiber, S. Avissar, A. Danon, R.H. Belmaker, *Biol. Psychiatry* 29 (1991) 273–280.
- [7] L.T. Young, P.P. Li, S.J. Kish, K.P. Siu, J.J. Warsh, *Brain Res.* 553 (1991) 323–326.
- [8] S. Avissar, G. Schreiber, A. Danon, R.H. Belmaker, *Nature* 331 (1988) 440–442.
- [9] N. Minadeo, B. Layden, L.V. Amari, V. Thomas, K. Radloff, C. Srinivasan, H.E. Hamm, D. Mota de Freitas, *Arch. Biochem. Biophys.* 388 (2001) 7–12.
- [10] P.C. Sternweis, *Curr. Opin. Cell Biol.* 6 (1994) 198–203.
- [11] A.G. Gilman, *Biosci. Rep.* 15 (1995) 65–97.
- [12] S. Rens-Domiano, H.E. Hamm, *FASEB J.* 9 (1995) 1059–1066.
- [13] A. Geisler, A. Mørk, R. Bach, V. Gallicchio (Eds.), *Lithium and Cell Physiology*, Springer-Verlag, New York, 1990.
- [14] S. Avissar, D.L. Murphy, G. Schreiber, *Biochem. Pharmacol.* 41 (1991) 171–175.
- [15] T.D. Ting, S.B. Goldin, Y.K. Ho, *Methods Neurosci.* 15 (1993) 180–195.
- [16] D.E. Coleman, A.M. Berghuis, E. Lee, M.E. Linder, A.G. Gilman, S.R. Sprang, *Science* 265 (1994) 1405–1412.
- [17] D.E. Coleman, E. Lee, M.B. Mixon, M.E. Linder, A.M. Berghuis, A.G. Gilman, S.R. Sprang, *J. Mol. Biol.* 238 (1994) 630–634.
- [18] F. Wittinghofer, J.C. Lascal, F. McCormick (Eds.), *The ras Superfamily of GTPases*, CRC Press, Boca Raton, 1993.
- [19] D.G. Lambright, J.P. Noel, H.E. Hamm, P.B. Sigler, *Nature* 369 (1994) 621–628.
- [20] M. Chabre, *TIBS* 12 (1987) 213–215.
- [21] D.E. Coleman, S.R. Sprang, *Biochemistry* 37 (1998) 14376–14385.
- [22] D.M. Bollag, S.J. Edelstein (Eds.), *Protein Methods*, Wiley-Liss, New York, 1991.
- [23] B.O. Fanger, *Anal. Biochem.* 162 (1987) 11–17.
- [24] G.W. Smithers, M. Poe, D.G. Latwesen, G.H. Reed, *Arch. Biochem. Biophys.* 280 (1990) 416–420.
- [25] K.P. Hofmann, D. Emeis, P. Schnetkamp, *Biochim. Biophys. Acta* 725 (1983) 60–70.
- [26] P.A. Hargrave, H.E. Hamm, K.P. Hofmann, *Bioessays* 15 (1993) 43–50.
- [27] T.L. James, J.H. Noggle, *Proc. Natl. Acad. Sci. USA* 62 (1969) 644–649.
- [28] K.A. Connors (Ed.), *Binding Constants*, John Wiley, New York, 1987.
- [29] D. Mota de Freitas, L. Amari, C. Srinivasan, Q. Rong, R. Ramasamy, A. Abraha, C.F.G.C. Geraldes, M.K. Boyd, *Biochemistry* 33 (1994) 4101–4110.
- [30] C. Srinivasan, N. Minadeo, J. Toon, D. Graham, D. Mota de Freitas, C.F.G.C. Geraldes, *J. Magn. Reson.* 140 (1999) 206–217.
- [31] W. Urry, L. Trapane, C.M. Venkatachlam, R.B. McMichens, *Methods Enzymol.* 171 (1989) 286–342.
- [32] B. Raju, E. Murphy, L.A. Levy, R.D. Hall, R.E. London, *Am. J. Physiol.* 256 (1989) C540–C548.
- [33] R.E. London, *Ann. Rev. Physiol.* 53 (1991) 241–258.
- [34] E. Murphy, R.E. London, *Methods Neurosci.* 27 (1995) 304–318.
- [35] L. Amari, B. Layden, Q. Rong, C.F.G.C. Geraldes, D. Mota de Freitas, *Anal. Biochem.* 272 (1999) 1–7.
- [36] A. Abraha, D. Mota de Freitas, M.M.C.A. Castro, C.F.G.C. Geraldes, *J. Inorg. Biochem.* 42 (1991) 191–198.
- [37] Q. Rong, D. Mota de Freitas, C.F.G.C. Geraldes, *Lithium* 3 (1992) 213–220.
- [38] Q. Rong, M. Espanol, D. Mota de Freitas, C.F.G.C. Geraldes, *Biochemistry* 32 (1993) 13490–13498.
- [39] Q. Rong, D. Mota de Freitas, C.F.G.C. Geraldes, *Lithium* 5 (1994) 147–156.
- [40] L. Amari, B. Layden, J. Nikolakopoulos, Q. Rong, D. Mota de Freitas, G. Baltazar, M.M.C.A. Castro, C.F.G.C. Geraldes, *Biophys. J.* 76 (1999) 2934–2942.
- [41] A. Mørk, A. Geisler, *Pharmacol. Toxicol.* 60 (1987) 241–248.
- [42] A. Mørk, A. Geisler, *Pharmacol. Toxicol.* 60 (1987) 17–23.
- [43] D. Mota de Freitas, *Methods Enzymol.* 227 (1993) 78–106.
- [44] R.A. Komoroski, *Magn. Reson. Imaging* 18 (2000) 103–116.
- [45] F.G. Ridell, *J. Inorg. Biochem.* 39 (1990) 187–192.
- [46] B.T. Layden, A.M. Abukhdeir, N. Williams, C.P. Fonseca, L. Carroll, M.M.C.A. Castro, C.F.G.C. Geraldes, F.B. Bryant, D. Mota de Freitas, *Biochem. Pharmacol.* 66 (2003) 1915–1924.